

Review

New Opportunities for Low Alloy Steels—Master Alloys for Liquid Phase Sintering

Mónica Campos ^{1,*} , José M. Torralba ^{2,*} , Raquel de Oro ³, Elena Bernardo ⁴ and Andrea Galán-Salazar ¹

¹ Materials Science and Engineering Department, Universidad Carlos III de Madrid, 28911 Leganés, Spain; agsalaza@ing.uc3m.es

² IMDEA Materials Institute, Universidad Carlos III de Madrid, 28903 Getafe, Spain

³ Institute of Chemical Technologies and Analytics, Technische Universität Wien, 1060 Vienna, Austria; raquel.oro.calderon@tuwien.ac.at

⁴ AMES PM Tech Center, 08620 Sant Vicenç dels Horts, Barcelona, Spain; elena.bernardo@ames.group

* Correspondence: campos@ing.uc3m.es (M.C.); torralba@ing.uc3m.es (J.M.T.)

Abstract: The Master-alloy (MA) alloy route to promote a liquid phase during sintering has great potential to reduce costs in low alloyed sintered steels, meanwhile enabling the introduction of innovative alloy systems with Cr, Mn and Si. However, in order to successfully modify the performance of steels, multi requirements must be met, including, for example, solubility with the base material, compatibility with the usual sintering atmospheres, homogeneous distribution of the powdered master alloy in the material and the control of secondary porosity. Efforts have been made to properly design the composition of MA, to identify the reducing agents and to understand how they affect the wetting and liquid spreading all over the sintered part. This work reviews these key aspects for the efficient development of steels and explores the possibility to achieve a composition that can act as liquid former or as sinter braze adapting its use to the component requirement.

Keywords: liquid phase sintering; master alloys; wettability; surface energy; sintered low alloyed steels



Citation: Campos, M.; Torralba, J.M.; Oro, R.d.; Bernardo, E.; Galán-Salazar, A. New Opportunities for Low Alloy Steels—Master Alloys for Liquid Phase Sintering. *Metals* **2021**, *11*, 176. <https://doi.org/10.3390/met11010176>

Received: 13 December 2020

Accepted: 14 January 2021

Published: 19 January 2021

Publisher's Note: MDPI stays neutral with regard to jurisdictional claims in published maps and institutional affiliations.



Copyright: © 2021 by the authors. Licensee MDPI, Basel, Switzerland. This article is an open access article distributed under the terms and conditions of the Creative Commons Attribution (CC BY) license (<https://creativecommons.org/licenses/by/4.0/>).

1. Introduction

The sintered steels industry has been in continuous evolution ever since in 1937 period General Motors introduced the first iron-based components manufactured by using powder metallurgy (PM) [1]. Today it can be found PM parts in many systems in a car: injection, engine, transmission, steering, brakes, air conditioning, electrical engines and so forth. Hence, many different compositions and processing routes have been developed and optimised in the last decades. The topic “low alloyed PM steels” covers many different compositions where the total amount of alloying elements remains under 7 wt.%, having a good compromise between the mechanical properties and the dimensional tolerances. It can be noted that conventional PM aims at obtaining near net shape components through the powder manufacturing route.

It should be noted that the main drawback of sintered components made using uniaxial pressing and sintering (P + S) is the limited capability because of plastic deformation of the parts due to the high level of porosity that remains in the part, which can be estimated to be between 5–10% in volume (Figure 1) [2]. Usually, PM parts do not need further processing steps where severe plastic deformation is involved and thus they are required to meet a certain density level. However, many technological improvements have been introduced in the past decades looking for an improvement in the density level of the PM steels or at least a modification in the size, distribution and amount of porosity, to improve the ductility without producing losses in the dimensional control which is one of the main advantages of the PM process [3–6].

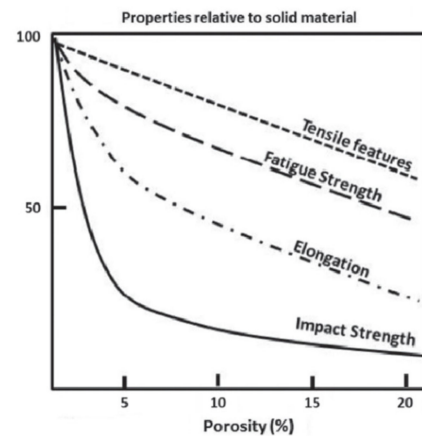


Figure 1. Effect of porosity on the main properties as a % of theoretical maximum [2].

These advances have contributed to the extended use of these steels as high quality structural materials (it has to be considered that the final density of the components has increased from $6.3 \text{ g}\cdot\text{cm}^{-3}$ to $7.4 \text{ g}\cdot\text{cm}^{-3}$ [7]). Nowadays, PM steels play an outstanding role in the automotive sector. The advanced balance between productivity, properties and cost that characterise this family of steels (in comparison with forged or cast steels) is one of the successful keys for this industry. Nevertheless, the demand for higher properties from the automotive sector drives the development of sintered steels for the production of new components with higher performance at lower costs.

To reach this objective, different strategies have been developed to improve the processing route, for instance, in the pressing step, the warm compaction process or the high velocity compaction and in the sintering step, the use of high temperature sintering [8–12]. But the development of new alloying systems is no doubt one of the most explored alternatives. In the evolution of new developed alloying systems, three turning points have allowed the advance of this family of materials:

1. The Cu addition to the Fe-C system in the late 1960s [2].
2. The diffusion alloying method in the CU-Ni-Mo systems in the 1980s [11].
3. The introduction of high oxygen affinity elements (Cr, Mn) between 1998–2003 [12].

The addition of cheaper alloying elements (compared to the conventional Cu or Ni), such as Cr, Mn or Si, provides an improvement in hardenability which is something really attractive. But the use of these elements requires technological improvements during sintering due to their high oxygen affinity and the need to avoid oxide formation, especially of some highly stable oxides. This fact has produced a reduced usage in the industry. From these three elements, Cr is the one which is used industrially as a pre-alloyed powder [9,11,13].

In order to provide the required combination of properties/cost, the sintered steel industry must come up with strategies to cope with problems related to high sensitivity to oxidation, the lack of homogeneity and the presence of porosity. Such problems are responsible for the decrease in properties and dimensional tolerances of today's steels and as a consequence, their service performance. Likewise, the high and unstable prizes of the current alloying elements and the need to use special manufacturing processes, are obstacles to their industrial growth.

Being more specific, the ways to improve these steels came, simultaneously, from the design of new alloying systems and a method for obtaining higher densities. Under this approach, the use of master alloys is one of the most suitable alternatives because it can act in the two ways, simultaneously [14]. In comparison to other alloying procedures such as the diffusion alloying powders or fully pre-alloyed powders, the master alloy route allows the retention of the high compressibility of the plain iron powder while also maintaining a high degree of homogenisation (for certain conditions). Nevertheless, the main

advantage of the master alloys is the flexibility to select the alloying system composition and the possibility of adjusting the composition design to the required specifications of the component.

The use of master alloys in the development of sintered steels has an extra advantage when the composition is designed with a melting point under the sintering temperature [15]. During sintering, the master alloy melts and produces a liquid phase which enhances the diffusion processes and reduces the porosity, while at the same time, helps to distribute the alloying elements. The use of these type of master alloys is not only a way to introduce the alloying elements but also a potential way to improve the density and the properties of the sintered steel. Nevertheless, it has been considered that the formation of a liquid phase during sintering poses new challenges related with the dimensional control, the secondary porosity or the possible reactivity with the solid phases. All these new challenges must be properly analysed with the objective of obtaining high performance materials.

Moreover, the introduction of master alloys allows a reduction in the total amount of alloying elements in the system. Today this strategy is a must to reduce costs. From this tendency, the concept of 'lean steels' emerged in the middle of the 2000's [16–18], meanwhile the prices of Ni and Mo rapidly increased [19]. This strategy has allowed the design of new steel grades with an optimised amount of alloying elements under 3 wt.%, with a good performance after sintering and/or heat treatment. The available tools to optimise the composition of the master alloy (based on a thermodynamic approach) allows the efficient use of the alloying elements and is a good way to produce a more economical and competitive products.

2. Evolution of Master Alloys

In the context of PM, a master alloy can be defined as:

“A powder with a high amount of potential alloying elements in PM steels designed to be mixed with a base powder, with the objective to provide a specific chemical composition which enables the achievement of a certain level of mechanical properties and a specific microstructure after the sintering process”.

This concept was firstly developed with the specific aim of introducing alloying elements with high affinity for oxygen, as their chemical activities can be reduced when added through an alloy or even, in the case of Mn avoiding sublimation [20]. But the objective of developing a liquid phase was not achieved. Initially, Cr, Mn, Si or V were considered as potential elements to be introduced as master alloys due to their excellent balance between cost and performance. Nevertheless, the master alloys concept brought an important challenge due to the technological barriers that were introduced.

Great efforts were made in the 1970s to design and optimise different master alloy compositions as a way to improve the mechanical properties and dimensional control of sintered steels. Figure 2 shows the evolution during the time of the main developed compositions and their manufacturing method. It can be seen that there were two periods, before the mid of the 1980s and from 1990. The introduction of the atomising route to produce master alloy powders and the compositional design using thermodynamical software, were the two main driving forces in their development.

The developments of master alloys for PM steels has been a research topic since the early 1970s. During the following two decades, different interesting master alloys, tagged as MCM (Mn-Cr-Mo), MVM (Mn-V-Mo) and MM (Mn-Mo), with the specific objective to obtain local hardenability and the development of non-equilibrium microstructures, were carefully studied [21–23]. Nevertheless, this idea was abandoned in the 1990s, mainly due to the two reasons: (1) the high sintering temperature required (near 1280 °C) to fully dissolve the carbides present in the master alloy particles and (2) the high level of wear in the pressing tools, due to the high hardness of the master alloy particles (produced at that time by casting and crushing).

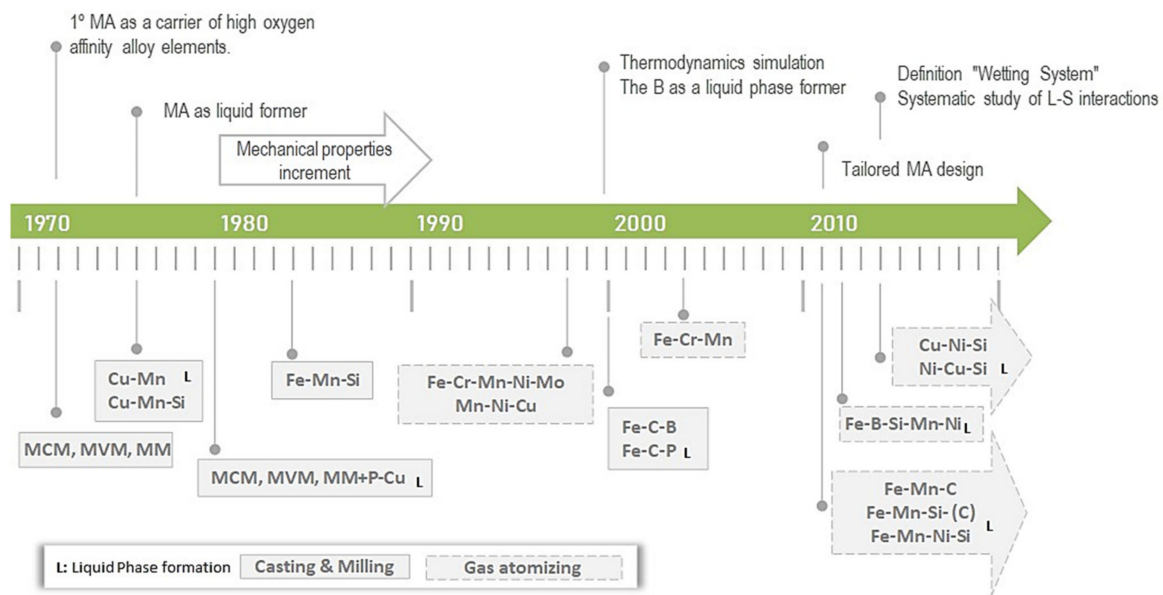


Figure 2. Evolution of the research paths in master alloys (MA) for sintered steels. The evolution has been monitored according to the pursuit of the objectives: (i) the introduction of elements with high affinity for the oxygen and/or (ii) the formation of a liquid phase.

Since that period, different compositions have been developed trying to pursue two objectives: the introduction of alloying elements with high oxygen affinity [21–26], the formation of a liquid phase during sintering [27–30] or the two objectives simultaneously [31–38] (Figure 2). But the main impetus for this research area took place in the late 1990s when two parallel developments became available. The first was the use of the inert gas atomizing systems as a production method for the master alloy powders (of small size and spherical shape, minimising the possible damage to the pressing tools). The second was the availability of powerful thermodynamic software tools that enabled the determination of compositions which allowed the production of liquid phases at the conventional industrial sintering temperatures [39,40]. The ultra-high pressure water atomizing system (UHPWA) allowed the production of spherical powders with low oxygen content ($\pm 1\%$), at low particle size ($d_{50} < 8 \mu\text{m}$) and small production costs, allowing new paths to the assumption of the master alloy route [41–43]. A reduction of particle size represents an advantage for the dimensional control of the sintered parts but also brings new challenges in the mixing and pressing steps which come from the difficulty in the handling and distribution of ultrafine powders.

In the past 10 years, new developments have contributed to the understanding of the master alloys as an efficient vehicle to modify the microstructure in sintered steels and the performance of the structural PM parts with a competitive cost. Two basic aspects have been developed:

1. The implementation of scientific methodology to design liquid phases with specific properties [15,44–48].
2. The systematic study of the solid-liquid interaction, the wetting system definition and the monitoring of the chemical processes that take place in the steels containing master alloys [49–56].

These concepts are highly associated with the development of four families of alloying systems: Fe-Mn-Si-(C-Cr); Fe-Mn-Si-Ni; Cu-Ni-Si and Ni-Cu-Si. The design of these alloys have been adapted to different requirements related to the sintering temperature, the steel microstructure or the dissolving character of the established liquid phase.

The studies were launched with systems of higher chemical compatibility and solving capability of Fe, Mn and Ni, with the aim to explore the routes of alloying element addition

through a liquid phase that would distribute and wet the solid particles, thus increasing the hardenability in the sintering necks which can be considered as the weak point of the sintered materials.

Afterwards, elements such as Cu, Ni or Mo, widely used in PM steels, have been considered as perfect candidates to design alternative master alloys compositions. In fact, master alloys made with these elements, in combination with some cheaper elements (but with high strengthening effect), are the driving force behind the development of new, efficient and economical alloy systems, providing higher hardenability at lower cost in standard sintering conditions. Here the objective is to combine the homogeneous distribution of the alloying elements with the higher densification when a liquid phase is present.

The last explored research line is to design a versatile composition that can easily distribute the alloying elements through liquid phase sintering but can also be used as a brazing alloy to join dissimilar components through a sinter-brazing process. In whichever direction, the design of the liquid phase is essential because the final properties of the component will be intimately linked to its wetting and infiltration capacity, the dimensional control of the liquid formed, the interaction between the solid and the liquid and, therefore, the dissolving character of the system. The composition can be designed to promote a liquid phase during the sintering process, therefore promoting the diffusion and densification mechanisms.

Amongst the design requirements, the compatibility of acting as filler alloy while sintering in commercial atmospheres can be incorporated. In this sense, steps in the processing route will be reduced, complying at the same time with the European directive RoHS2 [57] regarding the restriction of toxic substances.

3. Liquid Phase Sintering

Liquid phase sintering is a variant of the conventional solid-state sintering process. It entails the co-existence of a liquid phase with the solid particles for a certain time of period and at high temperature. The objective is to take advantage of the enhancement of the diffusion processes when a liquid phase is present. The main advantage of using a liquid phase during sintering is the activation of the sintering mechanism since mass transport is considerably faster in the liquid than in the solid phase. The liquid phase reduces friction between the solid particles and causes a rearrangement, which ultimately promotes rapid densification and elimination of porosity. In addition, a liquid phase favours the rapid alloying of the solid particles and in some specific systems (systems with Cu [58], Mo [59], Mo-B [60,61], Mn-Si [44], amongst others) it can act as an efficient way of distributing alloying elements and enhancing homogenisation in the steel.

The mutual solubility between liquid and solid governs the process, giving rise to the formation of either a permanent or a transient liquid phase. A permanent liquid phase implies that the liquid is constantly present while the process is at the maximum temperature. On the other hand, with a transitory liquid phase, the liquid varies its composition throughout the sintering process and is consumed by solid solution in the solid particles [62]. The solubility between solid and liquid also exerts an influence on the wettability of a certain system, that is, the ability of a liquid to propagate and spread over the surface of the solid phase. The main parameter characterising the wettability of a liquid is the contact angle θ formed between the liquid and the solid.

As shown in the diagram in Figure 3, three phases are involved in the wetting process: solid (S), liquid (L) and vapour (V). The angle formed in the solid-liquid interface and the tangent to the liquid-vapour interface at the triple point defines the contact angle, θ .

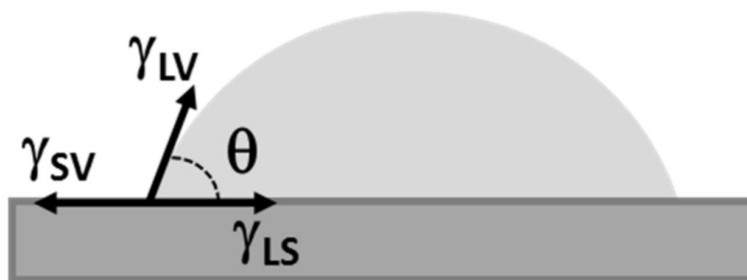


Figure 3. Representation of the process of wetting in the absence of interaction between the phases.

The magnitude of the contact angle depends on the balance between the interfacial energies present—solid-liquid interfacial energy γ_{SL} , liquid-vapour γ_{LV} and solid-vapour γ_{SV} . Contact angle values greater than 90° provide non-wetting conditions, while values lower than 90° relate to wetting conditions and favour the spreading of the liquid over the solid surface. In the simplest case, where the solid is rigid and homogeneous and there is no interaction between the phases, the contact angle θ is defined from the equilibrium between the interfacial energies. Considering the horizontal components, the Young's Equation (1) can be expressed [63]. According to this expression, for effective wetting of the liquid ($\theta < 90^\circ$), the difference $\gamma_{SV} - \gamma_{SL}$ must be positive.

$$\gamma_{SV} = \gamma_{SL} + \gamma_{LV} \cos \theta \quad (1)$$

However, in most solid-liquid systems at high temperatures, the spreading of the liquid is accompanied by dissolution, reaction, precipitation and so forth. Such phenomena lead to the modification (geometric and compositional) of the interface.

A solid-liquid system with good wettability favours the presence of a compressive capillary force that promotes the attraction among solid particles. The relationship between the wetting angle and the possibility of densification is represented in Figure 4, where the situation (a) favours the greatest attraction between the particles (low contact angle values) and the greatest degree of contraction, while the opposite situation (c) causes the separation of the particles and swelling in the system.

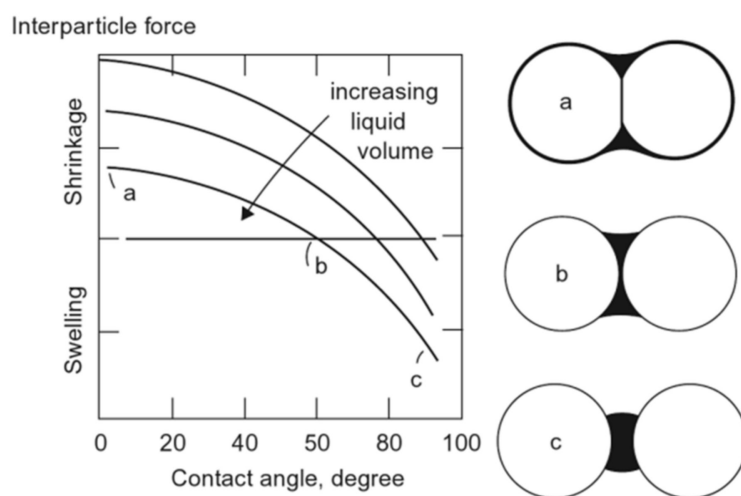


Figure 4. Relationship between wettability and densification capacity in a solid-liquid system: (a) represents excellent wettability and (c) lack of wettability, (b) is an intermediate stage. After [64].

4. Master Alloy Design Using Thermodynamic Software Tools

Approximately since the year 2000, the advance of master alloys has been closely associated with the use of computational calculations performed with thermodynamic software tools like ThermoCalc (Thermo-calc-software, Stockholm, Sweden) and kinetic modules like DICTRA (Thermo-calc-software, Stockholm, Sweden) [40,65,66]. Both programmes are based on the CALPHAD methodology (CALculation of PHase Diagrams), which offers a thermodynamic description using models of the Gibbs free energy of the phases that takes into consideration experimental data, mobility parameters and theoretical models and so forth, collected in databases. In this way, it is possible to find the phase diagram of complex systems by extrapolating/interpolating the data from the generally available binary or ternary systems.

The systematic search for eutectic compositions based on phase diagrams was first proposed by Du and Morral [39], in the quinary system Fe-Cr-Mo-V-C. The methodology developed is based on the combination of the projection of the liquidus univariate lines on a composition-composition diagram and on a temperature-composition diagram. As an example, Figure 5 shows a representation of the methodology followed for a ternary system A-B-C, with the two projections mentioned. A eutectic point is identified at the point of intersection of the three invariant lines. If this method is applied to a system of “n” components, a eutectic point will be defined considering the intersection of “n” invariant lines above this point. Gómez-Acebo et al. [40] applied this methodology to the system Fe-Cr-Mn-Mo-C and to the sets of binary, ternary and quaternary systems derived from it. When this type of simulation is used and once the candidate alloy is processed in the form of an ingot, the study should be completed with the experimental validation of the temperatures by means of differential thermal analysis (DTA) and metallography of the selected alloys.

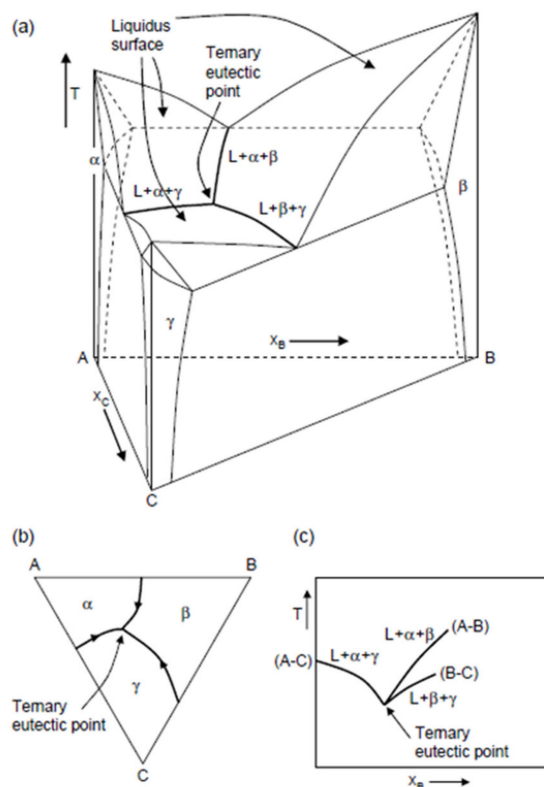


Figure 5. Different representations of a ternary diagram (a) 3-axes phase diagram of a ternary system, (b) projection of the liquidus univariate lines on a composition-composition diagram and (c) on a temperature-composition diagram after [40].

The thermodynamic aspects in the Fe-Mn-Si(-C) system have been studied in [44,67,68] by using various projections of the liquidus lines. Two compositions with a melting point below 1120 °C were selected—the eutectic Fe-38Mn-11Si ($T_{\text{melting}} = 1016$ °C) and the composition with incongruent melting Fe-39Mn-11Si-0.3C ($T_{\text{liquidus}} = 998$ °C, $\Delta T = 38$ °C). Thermodynamic software tools can calculate the sensitivity of the liquidus and solidus temperatures to the composition of the alloy. In that regard, C is the most critical element since an increase in C to above 1.5 wt.% causes an excessive increase of the liquidus temperature.

However, thermodynamic calculations are only the first step in a systematic study of the compositions, as explained in the flow chart in Figure 6. The methodology developed is based on three stages: after the first stage of theoretical description based on software tools, the alloy is processed into ingot form to carry out an experimental thermal validation by using differential thermal analysis (DTA), for example and metallography (Figure 6 right). Correspondingly, at this same stage, a macroscopic study of the wettability and infiltration of the liquid phases on Fe substrates and under different atmospheres (inert or reducing) is proposed. In the case of the MAs based on the Fe-Mn-Si(-C) system, these studies highlight the highly dissolutive character of the designed liquid phases, which is also corroborated with the kinetic study using the software DICTRA. The presence of these dissolutive processes is beneficial for the improvement of the wetting of the Fe particles. However, the main practical limitation of these alloys is their low (almost non-existent) distribution capacity. The microstructures of the steels modified with the Mn-Si master alloys illustrate the effect on the degree of homogenization that is achieved depending on the wettability, even at high temperature (1250 °C), where the formation of martensite is easily distinguishable in the areas with the highest concentration of alloying elements [28].

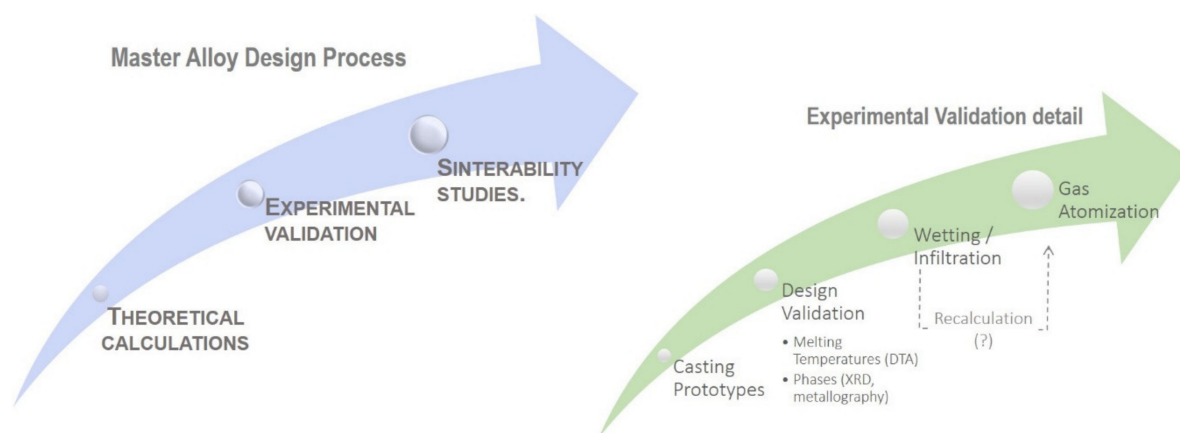


Figure 6. Master Alloy Design Process. **Left:** Design process for finding candidate compositions to promote liquid phase during sintering of low alloy steels. **Right:** Detail of the stages for the design of the composition [67,68].

After the atomization of selected MA compositions, sintering studies are carried out to evaluate the behaviour of the master alloys when incorporated into a mix together with Fe base powder and graphite. In this way, it is possible to evaluate mechanical properties, density, microstructure and so forth. of the sintered steel.

5. Interactions Phenomena in the Solid-Liquid System at High Temperatures

Reference [53] describes a model regarding the interactions that take place during the first stages of sintering. The wettability of a melted metal over a metal surface is only possible under specific superficial conditions. The reduction of oxides that naturally cover metallic surfaces must necessarily take place first in order to improve wetting conditions and allow wetting and dispersion of the liquid with low contact angles.

Previous results have revealed that favourable wetting conditions, in the absence of oxides that act as barriers, are favoured in the presence of different “actors” that are not

exclusively related to the pair solid/liquid or the interactions between them. Wettability should be considered as a property of a system (Figure 7) in which the environmental conditions (such as temperature, oxygen partial pressure, reduction potential of the atmosphere, composition of the atmosphere), interfacial reactions between the phases (solubility between the phases), chemical composition of the phases and the superficial conditions (oxides, coatings) are controlling factors with the same level of importance. The careful understanding of the interaction phenomena between the liquid and the atmosphere is a key factor to control wetting because it allows the change from an unfavourable wetting situation to a favourable one but also vice versa.

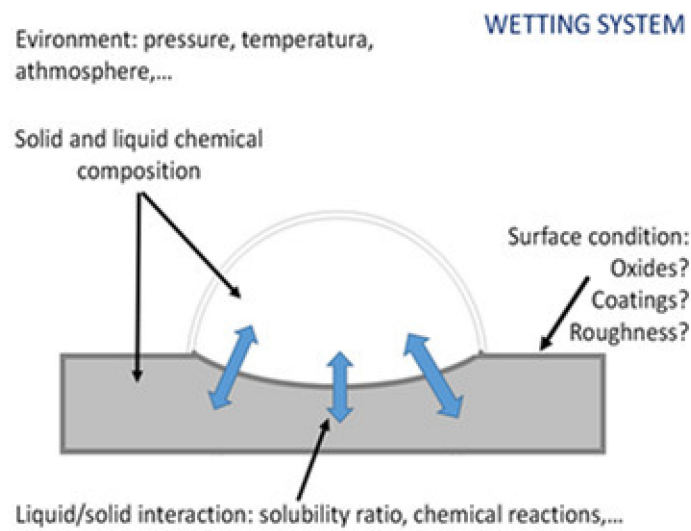


Figure 7. Wetting system that shows the main controlling agents of this process [53].

The metallic surfaces (both on the solid substrate and the liquid) are initially covered with an oxide layer. In the absence of reducing agents, the formed liquid is not able to wet the iron surface oxide as shown by liquid Cu on the Fe substrate in Ar (Figure 8). Only in presence of reducing agents, H_2 in the atmosphere (Figure 8a), Carbon in the composition of the substrate (Figure 8b) or Si as an element with higher oxygen affinity than the Cu or Fe (Figure 8c) the liquid phase wets and contact angle decreases.

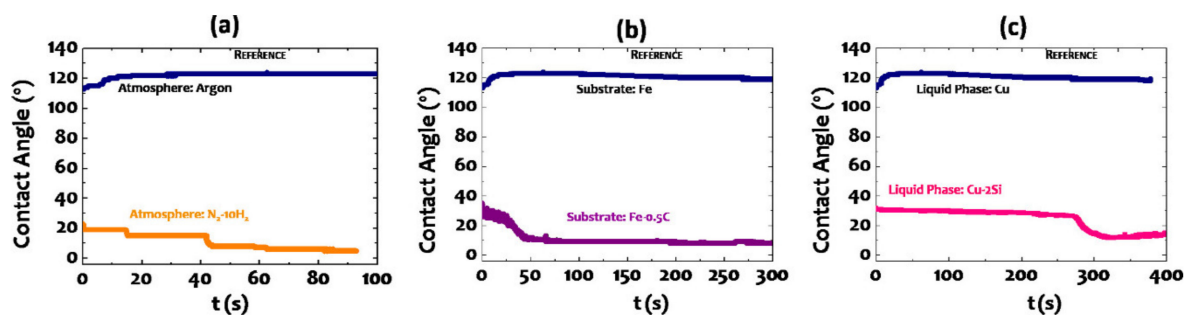


Figure 8. Influence of different parameters on the wetting behaviour of liquid Cu on Fe-based substrates: (a) influence of the atmosphere; (b) influence of the composition of the substrate Fe or Fe-0.5%C; (c) influence of the liquid –Cu or Cu-Si that assists the metallothermic reaction [53].

On the basis of the experimental results and the reported evidence [44,47,49], the model shown in Figure 9 is used to macroscopically illustrate how the propagation of the liquid could evolve from a non-wetting to a wetting situation in the presence of different reducing agents.

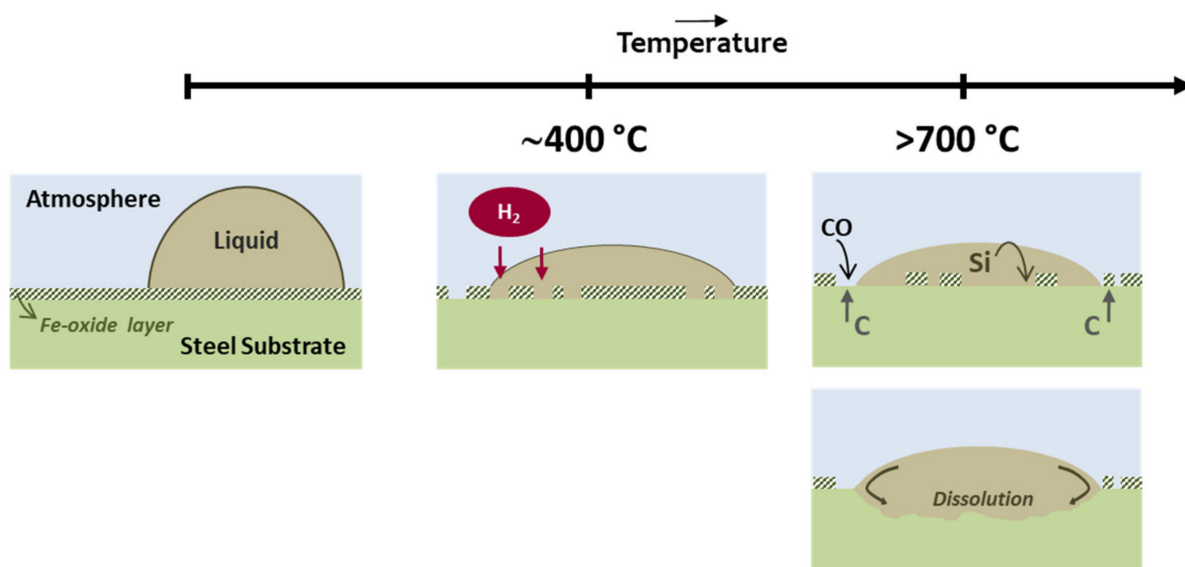


Figure 9. Scheme that illustrates the available reducing agents in a wetting system that contributes to the necessary reduction of surface oxides: at $400\text{ }^{\circ}\text{C}$ by H_2 present in the atmosphere and at higher temperatures by carbothermal reductions, metallothermic reactions and dissolution [53].

This situation is considered as the starting point with a drop that presents a high initial contact angle ($>90^{\circ}$) when it is in contact with the oxide of the iron surface (Figure 9). This scenario can be improved through two main mechanisms: the reduction of the oxide through the available reducing agents or the dissolution of the oxide in the liquid.

The reduction of the oxide is locally possible through solid and gaseous reducing agents that may be present in the atmosphere (H_2), the solid substrate (C), the liquid (Si) or may even be formed during the process (CO). Although their reduction potential when they serve as wetting agents seems to be similar since they promote a similar magnitude of improvement in the wettability capacity, they are sequentially activated with the increase in temperature. First, H_2 is able to reduce oxides at low temperatures, followed by the carbothermal (by C and CO) and metallothermic (Si) reactions at higher temperatures.

The dissolution mechanism not only depends on the temperature but also on the time of permanence of the liquid and the precipitation of secondary solid phases at the liquid/solid interface that can act as barriers for the progress of the dissolutive activity.

5.1. Oxidation-Reduction Phenomena in the Presence of a Liquid Phase

Although the role of the reducing agents has been concisely described, these phenomena have been thoroughly studied in [50,51]. Different characterisation techniques were used for this purpose, scanning electron microscopy, thermal analysis coupled with a mass spectrometer or XPS analysis which allows the identification of the chemical species present on the surface of the atomised master alloy powders (Figure 10). The X-ray Photoelectron Spectroscopy (XPS) is also known as ESCA (“Electron Spectroscopy for Chemical Analysis”). The principle of this technique is based in the ionisation of the atoms from the surface through X-ray radiation. One of the most important advantages is the possibility to identify (through high-resolution analysis) the different chemical states of the elements in regard to the kinetic energies of the emitted photoelectrons (Figure 10a). With the aim of understanding the chemical changes taking place on the surface as a consequence of the oxidation/reduction processes, the samples were submitted to different heating treatments.

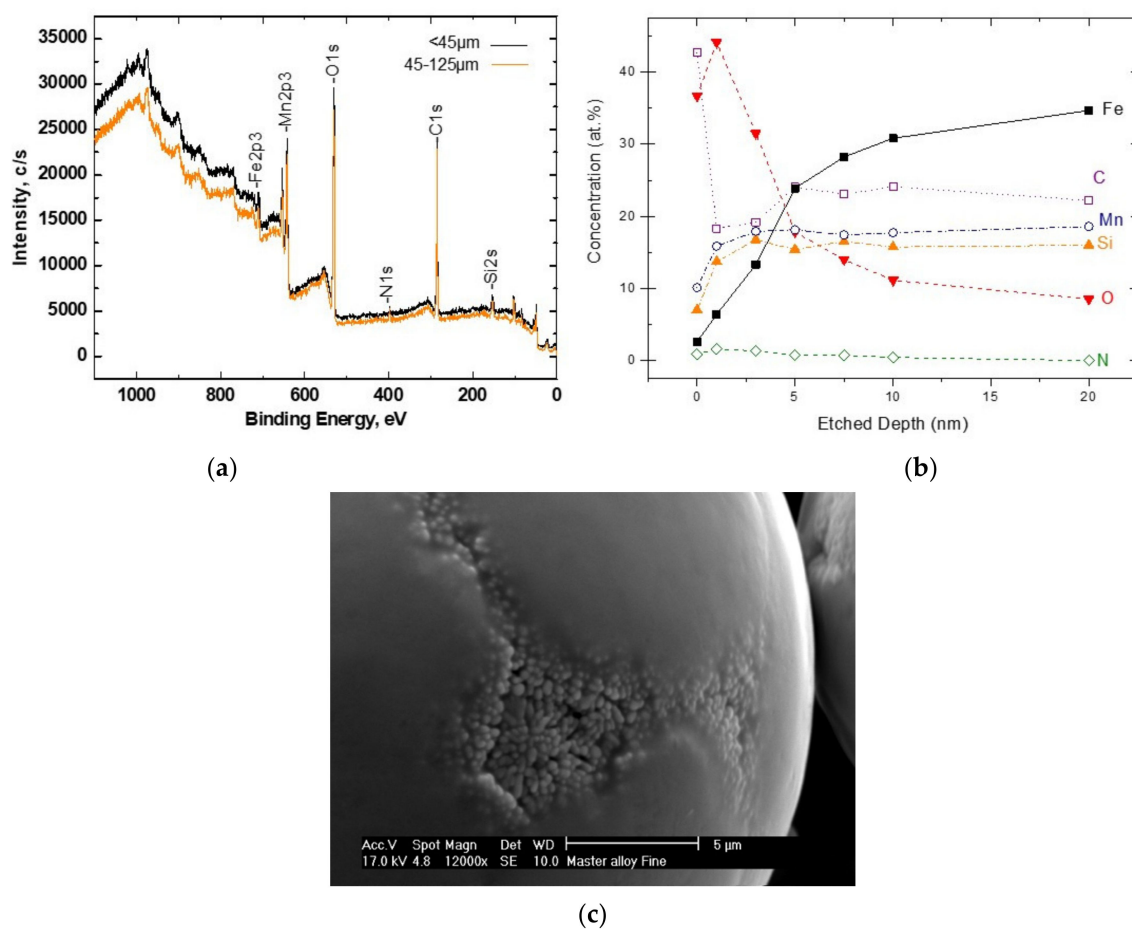


Figure 10. Surface Analyses on master alloy powder particles (a) The X-ray Photoelectron Spectroscopy (XPS) survey scan on the master alloy powder surface for two fractions of powder: <45 μm and 45–125 μm ; (b) Composition profile of the master alloy powder; (c) Scanning electron microscopy (SEM) image of the master alloy powder. Detailed image of the more stable particulate oxides [50].

The oxygen concentration decreases continuously with the sputter depth (Figure 10b). The high concentration of O in the outer powder layer reveals that the present oxides are mainly located in the surface of the master alloy. The oxygen concentration reaches a nearly constant value of 10 at.% at 20 nm depth. In the iron signal, the contribution of the metallic peak in the surface of the as-atomised powder represents 40% of the total peak-area and increases to 80% with only 1 nm etching. At 3 nm, the signal corresponds to the metallic state of Fe which indicates that the oxide layer covering the surface might be of approximately 1 nm depth (i.e., 1–2 monolayers).

The metallic contribution of Mn and Si increases rapidly when etching from 1 to 5 nm (Figure 10b). Afterwards, the growth rate is lower and at 20 nm depth, the oxide contribution is around 85% for both Mn and Si. According to these results, the stable oxide particles, rich in Mn and Si, might have a size below 7 nm.

Figure 10c shows a SEM image of the master alloy powder surface. Agglomerations of particulate oxide inclusions are present in specific areas of the powder surface. On the basis of the obtained information through XPS and SEM analysis, it can be concluded that the chemical composition of the master alloy particle surface is heterogeneous and might consist of a thin iron surface layer of around 1 nm depth, with areas containing agglomerations of Mn/Si particulate oxides below 7 nm.

Through thermal analysis techniques performed on steels containing master alloy additions, it is possible to measure (i.e., thermogravimetry) mass losses related to degassing

processes that take place under different atmospheres. Dilatometry studies are used to detect temperatures for the formation of the liquid phase, modification of the critical temperatures in the steel due to alloying and the dimensional stability of the sintered steel. When this technique is coupled with mass spectrometry, changes in the composition of the gases can be determined with the increase of temperature at the end of the furnace. These gases are formed as a result of oxidation/reduction processes that occur during the heating stage of sintering (see example in Figure 11).

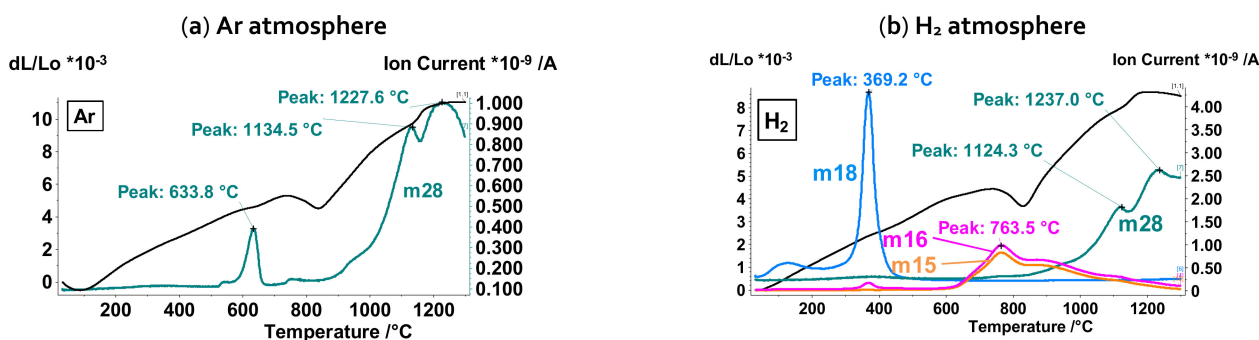


Figure 11. Dilatometry experiments coupled with mass spectrometry performed in green compacts that contain Fe-0.6%C-4%AM, studies in different atmospheres: (a) Inert: Ar and (b) Reducing: H₂.

In an Ar atmosphere (Figure 11a), the m28 (CO) curve shows that the first reduction processes take place at around 600–700 °C, corresponding to the reduction of less stable oxides (Fe oxides). Starting at approximately 1000 °C, there is a second reduction stage indicated by using a broad CO signal with peaks around 1100 and 1200 °C. This latter peak, related to the reduction of more stable oxides, is not completely registered even after reaching a temperature of 1300 °C (maximum temperature of the cycle), which indicates that the reduction is still not complete. In this case, the CO is the result of the carbothermal reaction, $\text{MeO} + \text{C} \longleftrightarrow \text{Me} + \text{CO}$. When sintering is performed in the presence of a H₂ reducing atmosphere (Figure 11b), iron oxides are reduced at temperatures around 400 °C as a result of the reaction with the H₂ from the atmosphere. In this case, the m18 (H₂O) signal, which has been formed through the following reduction reaction: $\text{Me}_x\text{O}_y + y\text{H}_2 \longleftrightarrow x\text{Me} + y\text{H}_2\text{O}$, is detected. The reduction of more stable oxides again takes place at high temperatures (1100–1200 °C) through the carbothermal reaction since carbon is the most effective reducing agent at higher temperatures. The reduction of more stable oxides is observed in the peak of the m28 signal that starts above 1000 °C and it is still present at a temperature of 1300 °C.

Sintering of steels containing master alloy additions in H₂ give rise to an interesting phenomenon that has never been detected before. At temperatures around 750 °C, the presence of a peak with mass m16 (CH₄) is detected. It is possible to state that this mass corresponds to methane because it is accompanied by a parallel curve of mass m15 (CH³⁺), an ionisation fragment that is always detected in the methane spectra. In this case, the composition of the master alloy only contains Si and after some calculations performed with the HSC Chemistry v4.1 software (HSC Chemistry, Tampere, Finland), it was possible to determine that the most probable reaction is $\text{Si} + 2\text{CO}(\text{g}) + 4\text{H}_2(\text{g}) \longleftrightarrow 2\text{CH}_4(\text{g}) + \text{SiO}_2$.

5.2. Analysis of Phase Solubility

The condition of solubility between the phases is decisive for the progress of sintering. The degree to which the chain of phenomena occurring during sintering, from solid particles rearrangement, densification, solution-precipitation, volume of formed liquid and the time of permanence of the liquid phase, is directly associated with the degree of solubility between the phases. At a given temperature, solubility in the system can be

expressed according to the solubility ratio S_R , which is calculated as the ratio between each of the solubilities [62]:

$$S_R = \frac{S_{S \rightarrow L}}{S_{L \rightarrow S}}, \quad (2)$$

where $S_{S \rightarrow L}$ represents the solubility of the solid in the liquid and $S_{L \rightarrow S}$ the solubility of the liquid in the solid.

When dealing with sintered systems with a permanent liquid phase, the solubility ratio is a determining factor in the evolution of sintering since it conditions the rearrangement phenomenon and therefore, the degree of achieved densification. A condition of unipolar solubility ($S_R \gg 1$) as represented in Figure 12a, that is, with a high solubility of the solid in the liquid and a limited solubility of the liquid in the solid, is the ideal condition to promote densification during sintering. As this condition is turned around, the densification capacity of the system is reduced and in the case of transitory liquid phases in which the solubility of the liquid in the solid is considerable, swelling occurs. This relationship between solubility and densification in the system is represented schematically in Figure 12b.

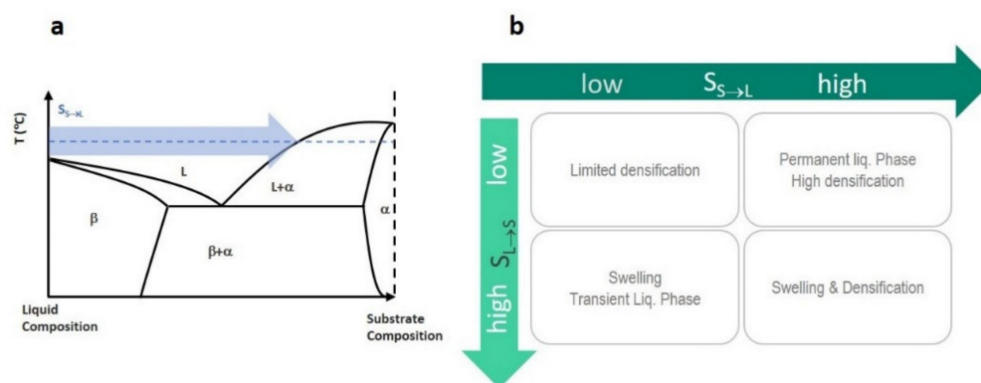


Figure 12. Solubility effects (a) Phase diagram representation with unipolar solubility and (b) relationship between solubility condition and tendency to densification/swelling [62].

In Table 1, different ferrous systems from the literature are shown. The influence of the solubility ratio on the dimensional behaviour of steel during sintering, shrinkage or swelling, is highlighted. Only the systems such as Fe-B or Fe-Ti with $S > 1$, give rise to shrinkage after sintering.

Table 1. Solubility effect on the dimensional behaviour during sintering of ferrous systems [62].

System	Solubility Ratio	Dimensional Effect
Fe-Al	0.02	swelling
Fe-Cu	0.07	swelling
Fe-Ti	3	shrinkage
Fe-B	7	shrinkage

However, this decisive parameter of S_R has not been applied to iron systems with transient liquid phases because the volume of liquid formed is considerably lower and there is a greater rigidity of the system. In [47], the effect of the liquid phase dissolving capacity on different variables was studied with dilatometric and sintering studies on a master alloy based on the Cu-Ni-Si system, designed for low alloyed sintered steels. The reported results are outlined in Figure 13.

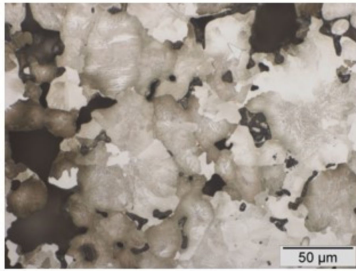
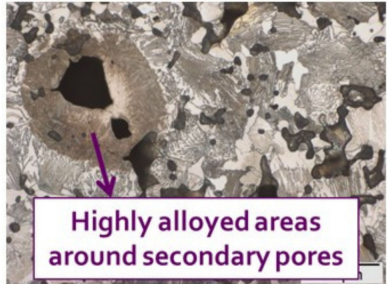
	Low dissolutive character	High dissolutive character
Wetting	Excellent	Excellent
Distribution	Excellent	Limited Prevalent dissolution of Fe
Microstructure		
Δ Dim	Sensitive to sintering conditions connected to SWELLING	Densification enhancer connected to SHRINKAGE

Figure 13. Properties map according to the nature of the dissolution [68].

With interrupted dilatometry, it is possible to study in-situ the phenomena that took place as the liquid was produced and the sintering progressed. The microstructural evolution of steels modified with Cu-Ni-Si based master alloys is presented in Figure 14. Low dissolution conditions (provided that good wettability exists) favour the rapid and homogeneous distribution of the liquid through the pore channels and between particle boundaries. It can be seen that as the temperature increases, the diffusion processes are activated. This favours the incorporation of the alloying elements into the Fe network and the reduction of the amount of free liquid in the microstructure. In the last stage (S4), once the sintering temperature has been reached, it can be seen how all the LP1 liquid has been practically consumed so that from this moment on sintering takes place in the solid state.

On the contrary, the presence of a liquid with a markedly dissolutive character (LP2) leads to a very different microstructural evolution. In the first moments of the formation of this liquid, the original master alloy particles are discerned. The liquid formed remains in the vicinity as it begins to dissolve the adjacent Fe particles. Due to the high dissolving character, this liquid is limited in its distribution capacity during the first sintering stage and consequently, favours the concentration of the alloying elements in the surroundings of the secondary pores. Thus, at the sintering temperature, extensive austenitic zones with a high concentration of alloying elements can be distinguished.

In both cases, the secondary porosity depends on the particle size in which the master alloy is incorporated.

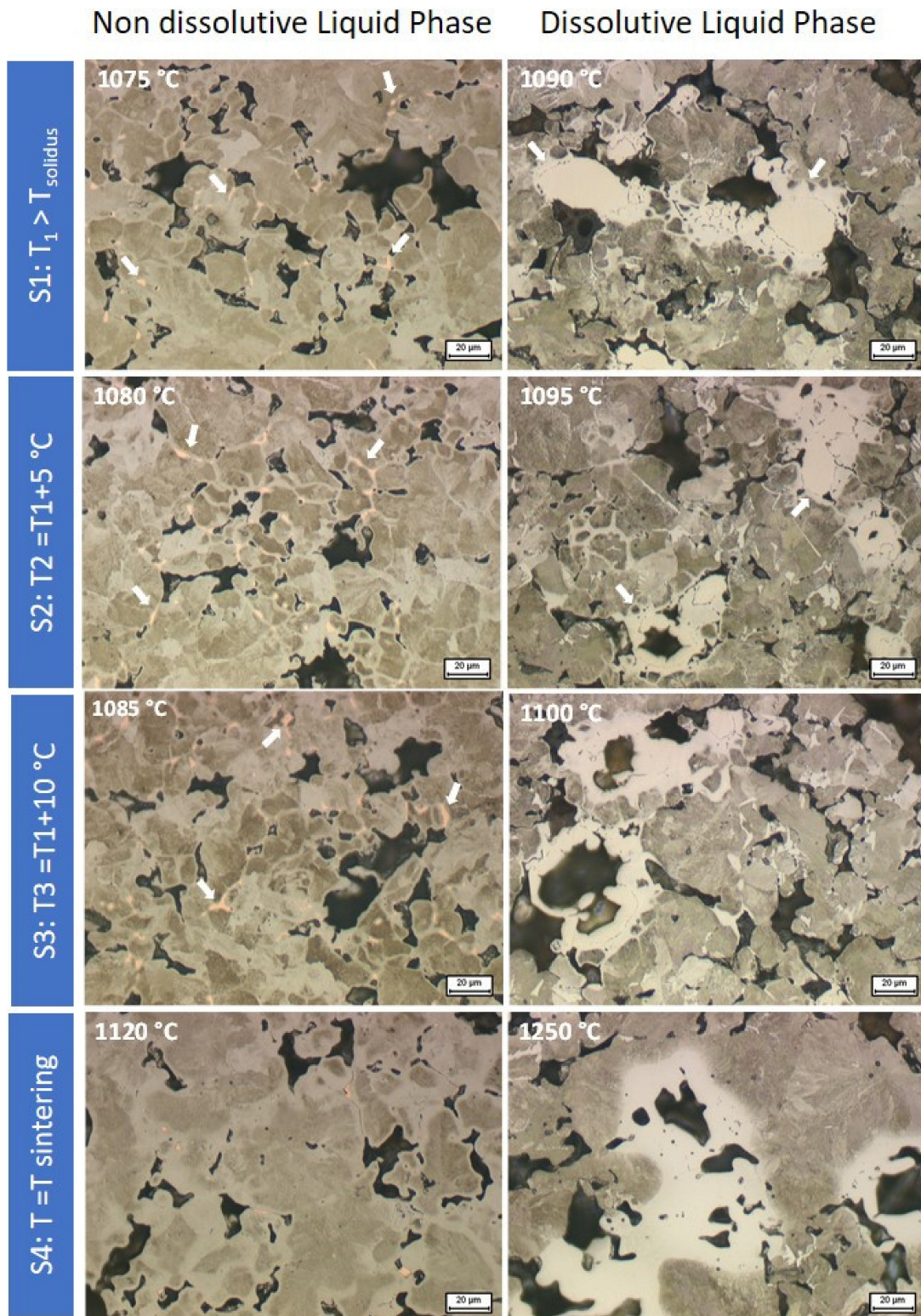


Figure 14. Microstructures of Fe-0.7%C steels modified by Cu-Mn-Si MA in each interrupted sintering stage, in Ar atmosphere and rapid cooling (100 °C/s) in the presence of: left, a non-dissolutive and right, dissolutive liquid phase.

In addition, the solubility between the phases plays a decisive role in the dimensional control of the sintered steel and in the densification degree. Poor dissolutive liquid phases and therefore with a high infiltration capacity, promote swelling of the final part because

of the penetration of the liquid through particles and grain boundaries, which cannot be compensated during the isothermal stage of the sintering process. However, the dissolving liquid phases promote ideal conditions for densification due to the reduced mobility of the liquid phase [47]. As a point to be highlighted, it is necessary to emphasise the possibility of designing “a la carte” by controlling this solubility parameter and adapting the microstructure of the steels to the final requirements. High solubility of Fe in the liquids (i.e., dissolvable liquid phases) will favour inhomogeneous microstructures with the presence of high hardenability phases around the largest pores, formed because of the melting of the MA particles during sintering. On the contrary, low-dissolvable liquid phases act as an effective distribution channel of the alloying elements in the steel.

6. Multiuse Liquid Phase Design

The first thing that must be defined is the requirements that this liquid phase should have in order to operate as a carrier of alloying elements contributing to the densification and on the other hand, as a liquid phase which provides a metallic bond between dissimilar substrates.

To be an appropriate alloying elements carrier phase, it must be formulated with a certain dissolving character, maintaining good wetting and allow the sintering necks to be reinforced by the presence of the alloying elements. It must be considered that there is also a close relationship between the wettability of the liquid phase formed and its welding capacity, as the liquid must be able to wet and spread on the solid surface ($\theta < 90^\circ$) to form a joint. In this context, the sintering atmosphere plays an essential role during the process, because it must reduce the surface oxides present, both in the substrates to be joined and in the filler material itself.

Furthermore, the value of the contact angle, as well as the relationship between the pressure that the atmosphere exerts on the substrates (P_{ext}) and the capillary force of the joint cavity (P_c), determine the formation of the meniscus at the edge of the joint which improves the resistance of the welded joint [69]. As shown in Figure 15, if the contact angle is less than 45° , the entire joint cavity is filled and a meniscus forms spontaneously outside the joint cavity and the thickness of the welding bead decreases as the external pressure and capillary force act in the same direction. However, when $45^\circ < \theta < 90^\circ$, the formed liquid remains inside the joint and does not form a meniscus if the external pressure is lower or equal to the capillary force. When the external pressure exceeds the capillary pressure, the liquid leaves the joint without being able to form a meniscus.

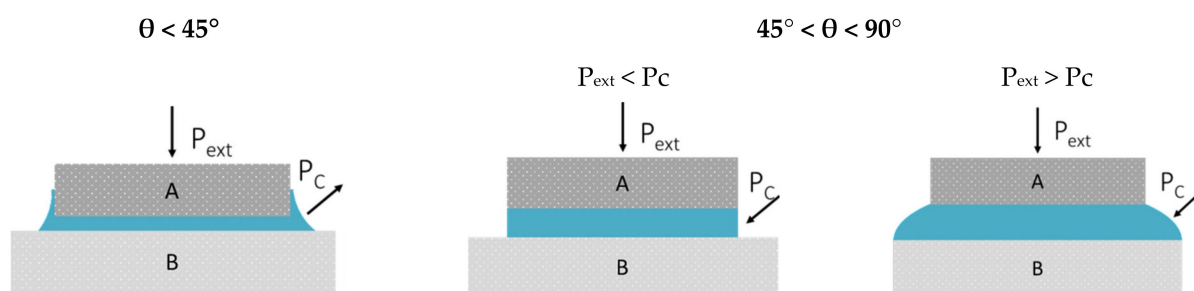


Figure 15. Relationship between wettability and weldability of the filler alloy P_{ext} is the pressure exerted by the atmosphere on the substrate, P_c is the capillary force of the joint cavity and θ wetting angle. From left to right, when the contact angle is less than 45° , the entire joint cavity is filled and when $45^\circ < \theta < 90^\circ$, the formed liquid remains inside the joint and does not form a meniscus if the external pressure is lower or equal to the capillary force. Adapted from [69].

On the other hand, the formation of a dissolving liquid able to close the surface porosity of the sintered component to be welded and avoid long infiltration distances, is required. However, an excessively dissolving liquid is not of interest either because it would distort the dimensional stability of the components to be joined and cause a large degree of erosion (that means surface dissolution). Due to the presence of a liquid

phase and the further generation of Marangoni flows, base material erosion occurs and the infiltration distance of the melt into the pores also contributes to the final erosion. Therefore, when designing the composition of the liquid phase to generate a joint with sinter bonding, a balance between wettability and dissolution must be reached.

From the point of view of joint integrity and mechanical behaviour of the final component, the formation of brittle phases in the joint or martensitic microstructures located in areas of high alloy concentration, must be avoided. To this end, one of the excluded alloying elements is B.

In this case the tests carried out with the sessile drop method have provided valuable information on the formation of the liquid [70,71]. Some differences were found between the experimental values of the solidus (1) and liquidus (2) temperatures and the simulated values calculated by ThermoCalc[®] (Figure 16). Thermodynamic calculations with existing databases can be complicated for systems with three or more elements in high proportions and there is also a limitation in the measurement of the contact angle because it is based on a morphological approach to the shape of the drop. On the other hand, the experimentally observed narrow range of melting corresponds to the rapid transformation from solid to liquid in the phase diagram and also means a rapid propagation of the liquid metal, which is one requirement for a good filler.

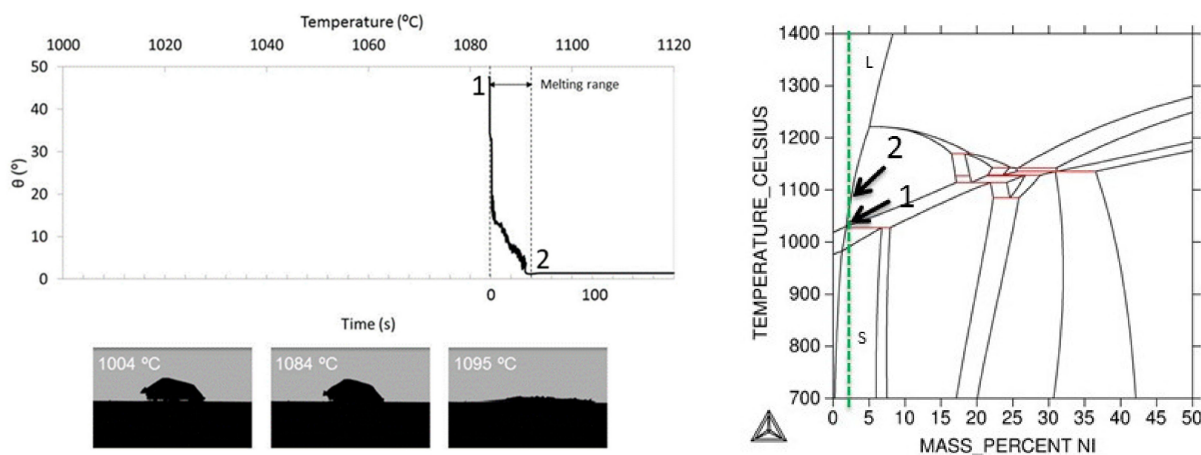


Figure 16. Relation between wetting experiments and phase diagrams. **Left:** Evolution of the contact angle on a dense Fe substrate in an Ar atmosphere. **Right:** Phase diagram (obtained with ThermoCalc[®] and the SSOL5 database).

The adaptability of the liquid phase designed is shown in Figure 17, which shows the ability to form the joint in completely different scenarios.

When one considers the mechanical response that a sintered steel, in which it has incorporated this liquid phase, would have as a vehicle carrying alloying elements and as a density modifier, the results are highly competitive (Figure 18). This shows the tensile strength of different steels against the percentage of alloying elements used. The data presented in Figure 18 correspond to steels with a density of around 7 g/cm³ and without any type of heat treatment. Both the data for low-temperature (1120 °C) and high-temperature (1250 °C) sintering are included where available.

It can be seen that the modified steels provide competitive tensile strengths with an alloying element content below 4%. Higher property levels with equivalent alloying element contents are only obtained with fully pre-alloyed commercial powders [72].



Figure 17. Bonding by sinter brazing of porous or dense substrates of different composition and/or manufacturing. Note the concave meniscus formed at the end of the joint. **Left:** powder metallurgy (PM) Steels, **Middle:** Dissimilar PM steels, **Right:** Dissimilar steels.

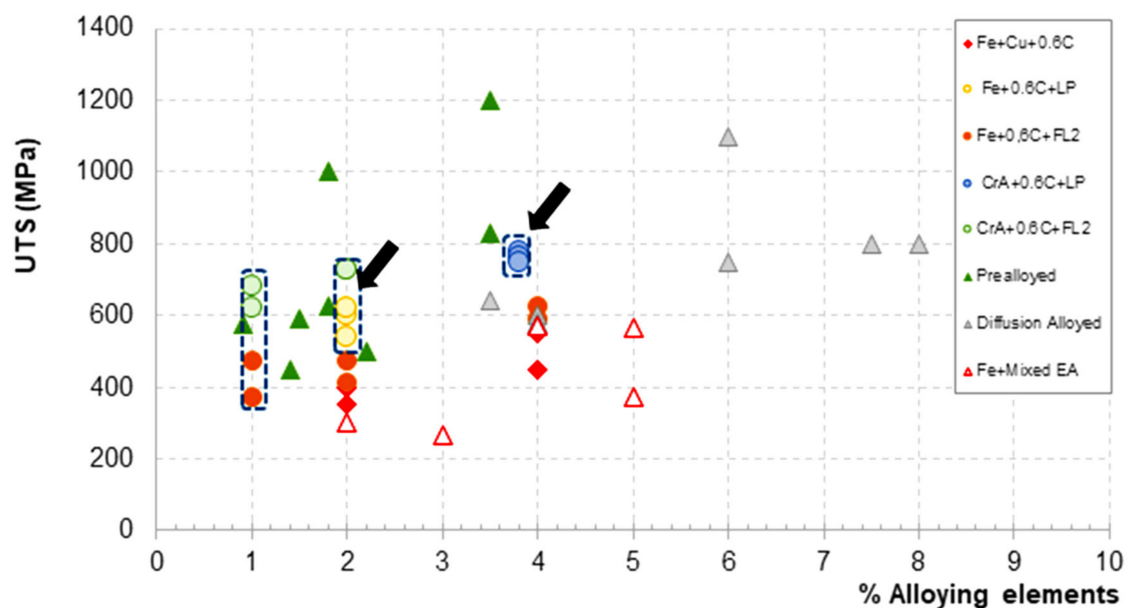


Figure 18. Ultimate tensile strength (UTS) versus % alloy elements (without carbon addition) for various commercial sintered steels [1] and for the modified steels of this work.

7. Conclusions

The correct design of master alloys using thermodynamic calculations in the first approximation, with the ThermoCalc software[®], provides a combination of properties that reaches or exceeds those obtained with commercial grades of powder. It requires quantities lower than 3% by weight of alloying elements, which are cost-effective and compatible with the most common sintering atmospheres.

The thermodynamic design provides for the choice of master alloy compositions that ensure the formation of a liquid phase at temperatures lower than the common sintering temperatures, thereby maintaining the dimensional stability of the component if the effects of all the reducing agents present are controlled. From the methodology described here, it should be noted that from preliminary stages of the design, it is possible

to predict the behaviour of the created liquid phase, which allows to discriminate and choose more precisely the composition of the MA and its influence on the properties and final microstructure of the steel.

Even multifunctional compositions can be chosen, which can be used as a master alloy or as a brazing alloy, with excellent wetting behaviour and with the advantage of being B-free (an element typically used in commercial compositions).

Thanks to this design strategy, it is possible to see the versatility that PM can offer by tailoring to the final performance by precisely modifying the microstructure of a commercial material through the design of the correct liquid phase.

Author Contributions: Conceptualization, M.C.; funding acquisition, J.M.T.; investigation, M.C., R.d.O., E.B. and A.G.-S.; methodology, M.C. and J.M.T.; supervision, M.C. and J.M.T.; writing—original draft, M.C.; writing—review & editing, J.M.T., R.d.O. and E.B. All authors have read and agreed to the published version of the manuscript.

Funding: This research was partially funded by Höganäs AB (Sweden) through the Höganäs Chair in Powder Metallurgy.

Institutional Review Board Statement: Not applicable.

Informed Consent Statement: Not applicable.

Data Availability Statement: Not applicable.

Conflicts of Interest: The authors declare no conflict of interest.

References

- Lindskog, P. The future of ferrous PM in Europe. *Powder Metall.* **2004**, *47*, 6–9. [[CrossRef](#)]
- Höganäs iron and steel powders for sintered components. In *Product Data Handbook: Powder Grades & Sintered Properties*; Höganäs AB: Höganäs, Sweden, 2002.
- Blanco, L.; Campos, M.; Torralba, J.M.; Klint, D. Quantitative evaluation of porosity effects in sintered and heat treated high performance steels. *Powder Metall.* **2005**, *48*, 315–322. [[CrossRef](#)]
- Dlapka, M.; Danninger, H.; Gierl, C.; Lindqvist, B. Defining the pores in PM components. *Met. Powder Rep.* **2010**, *65*, 30–33. [[CrossRef](#)]
- Danninger, H.; Jangg, G.; Weiss, B.; Stickler, R. Microstructure and mechanical properties of sintered iron. Part I: Basic considerations and review of literature. *Powder Metall. Int.* **1993**, *25*, 111–117.
- Danninger, H.; Jangg, G.; Weiss, B.; Stickler, R. Microstructure and mechanical properties of sintered iron. II: Experimental study. *Powder Metall. Int.* **1993**, *25*, 170–173.
- Tsutsui, T. *Technology Trend and Future Outlook of Structural Materials*; Hitachi Powdered Metals Technical: Tokyo, Japan, 2008; Volume 7.
- Torralba, J.M.; De Oro, R.; Campos, M. From sintered iron to high performance PM steels. *Mater. Sci. Forum* **2011**, *672*, 3–11. [[CrossRef](#)]
- Campos, M.; Blanco, L.; Sicre-Artalejo, J.; Torralba, J.M. High performance low alloy steels: Up date. *Rev. Metal.* **2008**, *44*, 5–12. [[CrossRef](#)]
- Narasimhan, K.S. Sintering of powder mixtures and the growth of ferrous powder metallurgy. *Mater. Chem. Phys.* **2001**, *67*, 56–65. [[CrossRef](#)]
- Danninger, H. New material systems and manufacturing techniques for high strength sintered precision parts. *Mater. Sci. Forum* **2003**, *426–432*, 115–122. [[CrossRef](#)]
- Lindskog, P. The history of Distaloy. *Powder Metall.* **2013**, *56*, 351–361. [[CrossRef](#)]
- Danninger, H.; Pötttschacher, R.; Bradac, S.; Šalák, A.; Seyrkammer, J. Comparison of Mn, Cr and Mo alloyed sintered steels prepared from elemental powders. *Powder Metall.* **2005**, *48*, 23–32. [[CrossRef](#)]
- Campos, M.; Sanchez, D.; Torralba, J.M. Sintering behaviour improvement of a low Cr-Mo prealloyed powder steel through Mn additions and others liquid phase promoters. *J. Mater. Process. Technol.* **2003**, *143–144*, 464–469. [[CrossRef](#)]
- Oro, R.; Bernardo, E.; Campos, M.; Gierl-Mayer, C.; Danninger, H.; Torralba, J.M. Liquid phases tailored for introducing oxidation-sensitive elements through the master alloy route. *Funtai Oyobi Fummatsumu Yakin/J. Jpn. Soc. Powder Metall.* **2016**, *63*, 172–184. [[CrossRef](#)]
- Yi, J.; Ye, T.; Peng, Y.; Xia, Q.; Wang, H. Sinter-Hardening process of PM steels and its recent developments. In *Proceedings of the Korean Powder Metallurgy Institute Conference, State Key Laboratory for Powder Metallurgy*; Central South University: Changsha, China, 2006; pp. 303–304.
- James, W.B. *Lean Hybrid Low-Alloy PM Molybdenum Steels*; Euro PM2009: Shrewsbury, UK, 2009; Volume 1, pp. 23–28.

18. Frykholm, R.; Bengtsson, S. New alloy designed for heat-treated applications. In Proceedings of the World Congress and Exhibition on Powder Metallurgy and Particulate Materials, Florence, Italy, 12 October 2010.
19. Markets. Available online: <https://www.mining.com/markets/> (accessed on 16 January 2021).
20. Šalák, A.; Selecká, M. *Manganese in Powder Metallurgy Steels*; Cambridge International Science Publishing Ltd.: Cambridge, UK, 2012.
21. Albano-Müller, L.; Thümmeler, F.; Zapf, G. High-Strength sintered iron-base alloys by using transition metal carbides. *Powder Metall.* **1973**, *16*, 236–256. [[CrossRef](#)]
22. Zapf, G.; Dalal, K. *Introduction of High Oxygen Affinity Elements Manganese, Chromium, and Vanadium in the Powder Metallurgy of P/M Parts*; Metal Powder Industries Federation: Princeton, NJ, USA, 1977.
23. Schlieper, G.; Thummler, F. High strength heat-treatable sintered steels containing manganese, chromium, vanadium and molybdenum. *Powder Metall. Int.* **1979**, *11*, 172–176.
24. Banerjee, S. New results in the master alloy concept for high strength sintered steels. *Prog. Powder Metall.* **1980**, *13*, 143–157.
25. Zhang, Z.; Sandström, R. Fe–Mn–Si master alloy steel by powder metallurgy processing. *J. Alloys Compd.* **2004**, *363*, 199–207. [[CrossRef](#)]
26. Beiss, P. Alloy cost optimization of high strength Mn–Cr–Mo steels with kerosene-atomized master alloy. In Proceedings of the Advances in Powder Metallurgy & Particulate Material, San Diego, CA, USA, 18–21 June 2006; pp. 12–20.
27. Khraisat, W.; Nyborg, L. Liquid phase sintering of ferrous powder by carbon and phosphorus control. *Powder Metall.* **2003**, *46*, 265–270. [[CrossRef](#)]
28. Xiu, Z.; Salwén, A.; Qin, X.; He, F.; Sun, X. Sintering behaviour of iron-molybdenum steels with the addition of Fe–B–C master alloy powders. *Powder Metall.* **2003**, *46*, 171–174. [[CrossRef](#)]
29. Xiu, M.Z. Effect of Fe–B and Fe–C master alloy powders on the liquid phase sintering of Fe–Mo–B–C sintered steels. *NTIS* **1995**, *97*, 102354.
30. Tojal, C.; Gómez-Acebo, T.; Castro, F. Development of PM stainless steels with improved properties through liquid phase sintering. *Mater. Sci. Forum* **2007**, *534–536*, 661–664. [[CrossRef](#)]
31. Fischmeister, H.F.; Larsson, L.-E. Fast diffusion alloying for powder forging using a liquid phase. *Powder Metall.* **1974**, *17*, 227–240. [[CrossRef](#)]
32. Fischmeister, H.; Drar, H. Zinc as an alloying element in Cu–Mn–Steel powder forgings produced by liquid-solid alloying. *Powder Metall. Int.* **1977**, *9*, 114–118.
33. Hamiuddin, M.; Upadhyaya, G.S. Effect of transition-metal carbides master alloy MCM on sintering of iron and iron-phosphorus powder premix. *Powder Metall. Int.* **1980**, *12*, 65–69.
34. Hamiuddin, M. Effect of copper addition on sintering of ternary iron powder premixes containing phosphorus. *Trans. Jpn. Inst. Met.* **1982**, *23*, 195–210. [[CrossRef](#)]
35. Klein, A.N.; Oberacker, R.; Thummler, F. High-Strength Si–Mn–Alloyed sintered steels—Microstructure and mechanical-properties I. *Powder Metall. Int.* **1985**, *17*, 13–16.
36. Klein, A.N.; Oberacker, R.; Thummler, F. High-Strength Si–Mn–Alloyed sintered steels—Microstructure and mechanical-properties II. *Powder Metall. Int.* **1985**, *17*, 71–74.
37. Sainz, S. Sinterability, hardenability and mechanical properties of Mn-containing PM steels through the use of a specially designed Fe–Mn–C master alloy. *Adv. Powder Metall. Part. Mater.* **2006**, *7*, 95–108.
38. Mocarski, S.; Hall, D.W.; Chernenkoff, R.A.; Yeager, D.A.; McHugh, C.O. Master alloys to obtain premixed hardenable powder metallurgy steels. *Powder Metall.* **1996**, *39*, 130–137. [[CrossRef](#)]
39. Du, H.; Morral, J.E. Prediction of the lowest melting point eutectic in the Fe–Cr–Mo–V–C system. *J. Alloy. Compd.* **1997**, *247*, 122–127. [[CrossRef](#)]
40. Gómez-Acebo, T.; Sarasola, M.; Castro, F. Systematic search of low melting point alloys in the Fe–Cr–Mn–Mo–C system. *Calphad* **2003**, *27*, 325–334. [[CrossRef](#)]
41. De Oro, R. New opportunities for master alloys: Ultra-High pressure water atomised powders. *Powder Metall. Rev.* **2019**, *8*, 55–66.
42. Oro, R.; Jalilizyaeian, M.; Dunkley, J.; Gierl-Mayer, C.; Danninger, H. New masteralloys for sintered high strength steels—The attractive route between mixing and prealloying. *Izv. vuzov. Poroshkovaya Metall. i funktsional'nye pokrytiya* **2018**, *4*, 15–27. [[CrossRef](#)]
43. De Oro Calderon, R.; Jalilizyaeian, M.; Dunkley, J.; Gierl-Mayer, C.; Danninger, H. New chances for the masteralloy approach. *Powder Metall. Prog.* **2018**, *18*, 121–127. [[CrossRef](#)]
44. Oro, R.; Campos, M.; Torralba, J.M.; Capdevila, C. Lean alloys in PM: From design to sintering performance. *Powder Metall.* **2012**, *55*, 294–301. [[CrossRef](#)]
45. Bernardo, E.; De Oro, R.; Campos, M.; Torralba, J.M. New findings on the wettability and spreading of copper on iron-base substrates. *Int. J. Powder Metall.* **2015**, *51*, 29–36.
46. Oro, R.; Bernardo, E.; Campos, M.; Gierl-Mayer, C.; Danninger, H.; Torralba, J.M. Tailoring master alloys for liquid phase sintering: Effect of introducing oxidation-sensitive elements. *Powder Metall.* **2015**, *59*, 31–40. [[CrossRef](#)]
47. Bernardo, E.; De Oro, R.; Campos, M.; Torralba, J.M. Design of low-melting point compositions suitable for transient liquid phase sintering of pm steels based on a thermodynamic and kinetic study. *Metall. Mater. Trans. Phys. Metall. Mater. Sci.* **2014**, *45*, 1748–1760. [[CrossRef](#)]

48. De Oro Calderon, R.; Bernardo, E.; Campos, M.; Gierl-Mayer, C.; Danninger, H.; Torralba, J.M. Master alloys for liquid phase sintering: Some key points for the design. *Met. Powder Rep.* **2016**, *71*, 184–192. [[CrossRef](#)]
49. Oro, R.; Campos, M.; Torralba, J.M. Study of high temperature wetting and infiltration for optimising liquid phase sintering in low alloy steels. *Powder Metall.* **2012**, *55*, 180–190. [[CrossRef](#)]
50. Oro, R.; Campos, M.; Hryha, E.; Torralba, J.M.; Nyborg, L. Surface phenomena during the early stages of sintering in steels modified with Fe-Mn-Si-C master alloys. *Mater. Charact.* **2013**, *86*, 80–91. [[CrossRef](#)]
51. Oro, R.; Hryha, E.; Campos, M.; Torralba, J.M. Effect of processing conditions on microstructural features in Mn-Si sintered steels. *Mater. Charact.* **2014**, *95*, 105–117. [[CrossRef](#)]
52. Oro, R.; Campos, M.; Gierl-Mayer, C.; Danninger, H.; Torralba, J.M. New alloying systems for sintered steels: Critical aspects of sintering behavior. *Metall. Mater. Trans. Phys. Metall. Mater. Sci.* **2015**, *46*, 1349–1359. [[CrossRef](#)]
53. Bernardo, E.; Oro, R.; Campos, M.; Torralba, J.M. Wetting phenomena for liquid Cu and Cu alloys on Fe-base substrate. *Adv. Powder Technol.* **2016**, *27*, 1027–1035. [[CrossRef](#)]
54. Gierl-Mayer, C.; de Oro Calderon, R.; Danninger, H. The role of oxygen transfer in sintering of low alloy steel powder compacts: A review of the “Internal Getter” effect. *JOM* **2016**, *68*, 920–927. [[CrossRef](#)]
55. De Oro Calderon, R.; Gierl-Mayer, C.; Danninger, H. Application of thermal analysis techniques to study the oxidation/reduction phenomena during sintering of steels containing oxygen-sensitive alloying elements. *J. Therm. Anal. Calorim.* **2017**, *127*, 91–105. [[CrossRef](#)]
56. Oro Calderon, R.; Gierl-Mayer, C.; Danninger, H. Effect of H₂ atmospheres on sintering of steels containing oxidation-sensitive elements introduced through the master-alloy route. *Int. J. Powder Metall.* **2017**, *53*, 31–40.
57. CE Marking European Commission OHS2 Directive 2011/65/EU. 2014. Available online: <https://eur-lex.europa.eu/legal-content/EN/TXT/?uri=CELEX%3A32011L0065&qid=1610956982477> (accessed on 18 January 2021).
58. Jamil, S.J.; Chadwick, G.A. Investigation and analysis of liquid phase sintering of Fe–Cu and Fe–Cu–C compacts. *Powder Metall.* **1985**, *28*, 65–71. [[CrossRef](#)]
59. Danninger, H. Sintering of Mo alloyed P/M structural steels. *Powder Metall. Int.* **1988**, *20*, 7–11.
60. Selecká, M.; Šalák, A.; Danninger, H. The effect of boron liquid phase sintering on properties of Ni-, Mo- and Cr-alloyed structural steels. *J. Mater. Process. Technol.* **2003**, *141*, 910–915. [[CrossRef](#)]
61. Sarasola, M.; Gómez-Acebo, T.; Castro, F. Microstructural development during liquid phase sintering of Fe and Fe–Mo alloys containing elemental boron additions. *Powder Metall.* **2005**, *48*, 59–67. [[CrossRef](#)]
62. German, R.M.; Suri, P.; Park, S.J. Review: Liquid phase sintering. *J. Mater. Sci.* **2009**, *44*, 1–39. [[CrossRef](#)]
63. Eustathopoulos, N. Dynamics of wetting in reactive metal/ceramic systems. *Acta Mater.* **1998**, *46*, 2319–2327. [[CrossRef](#)]
64. German, R.M. *Sintering: From Empirical Observations to Scientific Principles*; Elsevier Science: Amsterdam, The Netherlands, 2014.
65. Shi, P.; Engström, A.; Höglund, L.; Chen, Q.; Sundman, B.; Ågren, J.; Hillert, M. computational thermodynamics and kinetics in materials modelling and simulations. *J. Iron Steel Res. Int.* **2007**, *14*, 210–215. [[CrossRef](#)]
66. Andersson, J.-O.; Helander, T.; Höglund, L.; Shi, P.; Sundman, B. Thermo-Calc & DICTRA, computational tools for materials science. *Calphad* **2002**, *26*, 273–312. [[CrossRef](#)]
67. Oro, R. *Design of Master Alloys for Liquid Phase Sintering of Mn-Si Steels*; Universidad Carlos III de Madrid: Madrid, Spain, 2012.
68. Bernardo, E. *Optimization of Liquid Phases for Sintering Low Alloy Steels: Effect on Microstructure and Dimensional Control*; Universidad Carlos III de Madrid: Madrid, Spain, 2014.
69. Eustathopoulos, N.; Hodaj, F.; Kozlova, O. 1—The wetting process in brazing. In *Woodhead Publishing Series in Welding and Other Joining Technologies*; Sekulić, D.P., Ed.; Woodhead Publishing: Cambridge, UK, 2013; pp. 3–30. ISBN 978-0-85709-423-0.
70. Galán-Salazar, A.; Campos, M.; Torralba, J.M.; Kjellén, L.; Mårs, O. The base material: A key factor in sinter-brazing. *Met. Powder Rep.* **2016**. [[CrossRef](#)]
71. Galán-Salazar, A.; Campos, M.; Torralba, J.M.; Kjellén, L.; Mårs, O. Wettability for understanding the behaviour of new filler materials for sinter-brazing. *Powder Metall.* **2017**, *60*, 97–104. [[CrossRef](#)]
72. Galán-Salazar, A.; Campos, M.; Torralba, J.M. Novel multiuse liquid phase promoter for PM components. *J. Am. Ceram. Soc.* **2019**, *102*, 5691–5698. [[CrossRef](#)]